Bio-Based Upcycling of Poly(ethylene terephthalate) Waste for the Preparation of High-Performance Thermoplastic Copolyesters

Macromolecules

pubs.acs.org/Macromolecules Article

Bio-Based Upcycling of Poly(ethylene terephthalate) Waste for the Preparation of High-Performance Thermoplastic Copolyesters

Apostolos A. Karanastasis, Victoria Safin, and Louis M. Pitet*

Cite This: *Macromolecules* 2022, 55, 1042−1049 Read Online

ACCESS | Metrics & More | Article Recommendations | Supporting Information

ABSTRACT: Thermoplastic copolyesters occupy an important segment in the materials market, finding use in a wide range of engineering plastic applications. This fact owes itself to the versatility underlying the synthetic preparation. However, the industry relies nearly exclusively on virgin feedstocks that are derived from fossil-based resources. With a keen interest in improving the deleterious environmental impact of this material class, we combine postconsumer recycled PET (rPET) with a bioderived dimer fatty acid (DFA) building block for the synthesis of segmented thermoplastic copolyesters (TPCs) via solvent-free melt polycondensation. The influence of (i) catalyst type, (ii) hard block (i.e., PET) precursor, and (iii) soft block (i.e., DFA) content on the microstructure and mechanical properties of TPCs was assessed. Samples that exhibit equivalent mechanical strength and segment distribution are accessible using either pristine bis-hydroxy ethylene terephthalate (BHET) or rPET as starting materials. Screening of reaction conditions and composition space within this context was performed with small-scale (2 g) reactions. Further optimization of reaction conditions in terms of catalyst concentration and ethylene glycol deconstruction agent content allowed for the upscaled synthesis (100 g) of engineering-grade TPCs in a custom-built reactor. We believe that our results contribute to a new paradigm in the efforts for more responsible manufacturing practices for TPCs and provide an additional outlet for the efficient handling of end-of-life, recyclable plastics.

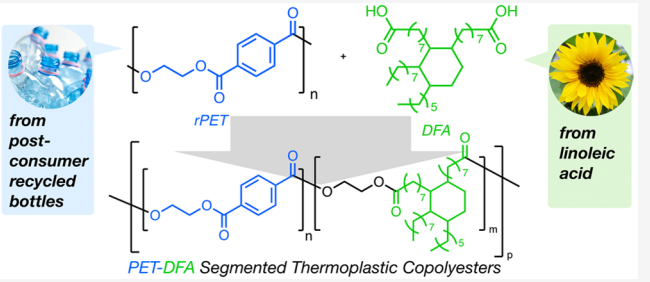

INTRODUCTION

Poly(ethylene terephthalate) (PET) is a commodity polymer with an outstanding array of properties that include very good mechanical strength, fracture resistance, thermal stability, extrudability, and very low gas (CO_2, O_2) permeability. The most notable applications for PET are beverage bottles, packaging, and textile fibers, which collectively account for more than 90% of global production. Eventually, the majority of postconsumer PET ends up being incinerated or persists in landfills for many generations.[1] After leaching into marine environments, PET can dwell as a microplastic pollutant.[2] While our understanding of the toxic effects of lower-molar-mass PET degradation byproducts on aquatic life is still very limited, it is certainly a potential cause for concern.[3] Currently, the mechanical recycling of PET is the main method of retaining the carbon in the manufacturing loop, albeit at relatively low rates.[4] A major barrier to improved recycling rates includes contamination of output streams due to inefficient sorting and the thermomechanical degradation of polymer chains during the typically high-temperature (>200 °C) melt reprocessing.

The development of new strategies for handling end-of-life PET has gained traction in recent years, in line with the ambitious sustainability targets set by international legislative bodies.[5] Chemical recycling technology of converting PET back to monomers, namely, terephthalic acid (TA) and ethylene glycol (EG), or to alkyl glycol derivatives, is mature in the pilot scale and breakthroughs of economic viability for industrial production are clear on the horizon.[6−10] The interested reader can refer to recent comprehensive reviews that cover the state-of-the-art in the chemical recycling of plastics[11,12] and in particular PET.[13,14]

Separately, the chemical repurposing of postconsumer plastics into materials with higher added value, referred to generally as upcycling, is also garnering attention. To date, PET upcycling protocols have mainly afforded niche small molecules[15−18] and micro/nanostructured carbon allotropes.[19−23] In upcycling studies where the objective was the preparation of macromolecular materials, PET has been treated as a digestible intermediate in multistep sequential processes. Following this approach, polyhydroxyalkanoates (PHA),[24] poly(amide urethanes),[24] polyionenes,[25] polyurethanes,[26] and polyesteramides[27] have been reported through metabolic or aminolytic pathways. While it is noteworthy that in a nascent

Received: November 11, 2021
Revised: January 3, 2022
Published: January 21, 2022

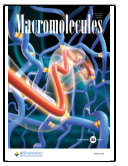

https://doi.org/10.1021/acs.macromol.1c02338
Macromolecules 2022, 55, 1042−1049

Scheme 1. Complementary Synthetic Pathways A and B to Afford PET-DFA TPCs from the Combination of DFA with Either (A) BHET or (B) rPET Precursors

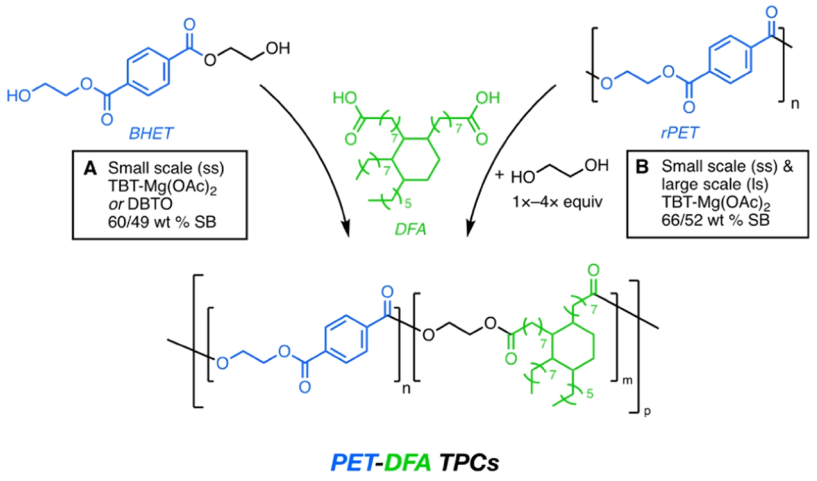

report, Papke and Karger-Kocsis[28] have envisioned the direct upcycling of PET refuse as a blended constituent in thermoplastic elastomer formulations, and Gioia et al.[29] deconstructed rPET in the presence of isosorbide for the preparation of a polyester precursor for coating applications, we could not find studies where PET was directly transformed into high-molar-mass polymers with useful thermomechanical properties.

Thermoplastic copolyesters (TPCs) constitute a materials class with commercial relevance, employed in demanding engineering applications[30] where the combination of thermal stability, chemical and abrasion resistance, and mechanical strength are critical. The molecular microstructure is described by the alternation of immiscible hard and soft segments (i.e., blocks) linked with ester bonds. Conventional hard blocks comprise rigid, semiaromatic repeat units, while the soft blocks typically contain bulky aliphatic or polyether polyol precursors. The favorable properties of the TPCs stem from the presence of segregated nanodomains of the hard, usually semicrystalline phase, embedded within a continuous amorphous phase comprising soft, flexible segments. The stoichiometric ratio between the hard and soft phase, the length of the soft block precursor, and the chemical composition of the blocks are synthetic handles that allow us to fine-tune the TPCs' bulk properties.

The synthesis and properties of TPCs comprising hard (i.e., semicrystalline) alkyl terephthalate units and soft blocks based on DFA derivatives (e.g., acids or diols) have been explored in the literature.[31−36] Nevertheless, these materials have been generated exclusively from virgin monomer feeds (i.e., dimethyl terephthalate, ethylene glycol, DFA). The most relevant reports to date are a patent[37,38] and a recent publication[39] that disclose the multistep preparation of polyol oligomers from rPET and DFAs intended as precursors to polyurethanes. Here, we report on the direct, one-pot upcycling of postconsumer recycled PET (rPET) into segmented TPCs using the renewable dimer fatty acid (DFA) Pripol 1009 as the soft building block. We initially prove the upcycling of rPET in the small-scale (ss ∼2 g) via a continuous one-pot deconstruction/polycondensation reaction and further optimize conditions for the multigram, large-scale (ls ∼100 g) batch preparation in a custom-built reactor. Our results show that the one-step deconstruction of rPET in the presence of a renewable diacid monomer leads to engineering-grade TPCs, provided excess diol (e.g., ethylene glycol) is dosed in the reaction mixture. We show that thermomechanical properties are consistent with a segmented copolyester architecture and are directly comparable with those of commercially available analogues, albeit with substantially slower crystallization rates as a consequence of the PET block.

RESULTS AND DISCUSSION

DFA is commercially available on large scale from Croda under the trade name Pripol 1009. It is a bio-based aliphatic building block ultimately derived from linoleic acid, which has various natural sources including sunflowers and safflowers. Pripol 1009 contains small amounts of isomers, but the primary component is an aliphatic cyclic compound. It contains two carboxylic acid functional groups per molecule and is consequently amenable to esterification, which was leveraged to react with either bis-hydroxy ethylene terephthalate (BHET) or rPET (Scheme 1). We set out to investigate the utility of DFA as a precursor to making TPCs from recycled PET. The initial task was to evaluate whether chemical recycling (e.g., glycolysis) to form a monomeric starting material such as BHET is a prerequisite for the PET component (Scheme 1, path A). On the contrary, we surmised that it may be possible to access segmented TPCs by reacting DFA directly with high-molar-mass rPET recyclate (Scheme 1, path B). BHET was sourced commercially but could be obtained in practice from the glycolysis depolymerization of high-molar-mass PET. The rPET used here was supplied by Cumapol and was exclusively sourced from postconsumer bottle-grade PET flake. As such, it has a relatively high molar mass (intrinsic viscosity ∼ 0.65 dL/g; M_n ∼ 25 kg/mol). Combining these ingredients with a suitable catalyst will presumably lead to transesterification, ultimately liberating ethylene glycol, which is removed under vacuum. The equilibrium reaction is driven forward by the removal of EG, accompanied by an increase in molar mass in a step-growth polycondensation and generating a multisegmented copolymer architecture with composition dictated by the feed ratio. The segments consist of alternating hard blocks (PET) and soft blocks (DFA), providing a range of mechanical properties depending on the relative content.

https://doi.org/10.1021/acs.macromol.1c02338
Macromolecules 2022, 55, 1042−1049

Small-scale (2 g) melt polycondensation was initially used to generate a series of these sustainable alternatives to conventional TPCs with a range of mechanical properties, in which several key reaction conditions were systematically evaluated. The first objective was to ascertain the influence of the hard block precursor on the final mechanical properties of the TPCs, whereby two different raw materials were explored. In one case, BHET was employed as a hard block precursor (Scheme 1, path A). Notably, reaction path A intrinsically contains an excess of EG within the BHET itself. A portion of the excess EG becomes a structural counterpart within the soft-segment DFA repeating unit as a virtue of the diacid functionality in the DFA monomer. The remaining excess EG is driven off as condensate during conversion to polymer and associated molar mass increase.

In parallel, high-molar-mass rPET pellets/nurdles (bottle-grade) were used as a direct input (Scheme 1, path B). The repeating unit structure of the final TPC is a crucial design parameter for reaction path B. Specifically, when using high-molar-mass rPET as a feedstock, excess EG must be added, which serves two purposes. EG becomes a structural component in the DFA-based repeating unit and also promotes mixing and extensive transesterification and subsequent redistribution of the ethylene terephthalate repeating units. It was initially surmised that the *in situ* glycolytic deconstruction of rPET and subsequent polycondensation of the digested intermediate in the presence of DFA should yield materials that are essentially equivalent to those obtained by the traditional two-step transesterification/polycondensation scheme that is employed for the BHET-based route. Importantly, in both reaction pathways, the complementary acid functionality of the DFA soft block readily reacts with the excess hydroxyl groups associated with the EG fragments and oligomer end-groups. In this manner, the Pripol DFA is covalently incorporated into the main chain of the growing oligomers.

For path A, we initially applied a 2 × 2 full factorial design to assess the influence of high (60 wt %) and low (49 wt %) target soft block content on the thermomechanical properties of the resultant TPCs. This was done in conjunction with investigating two industrially relevant catalytic systems based on either tetrabutyl titanate/magnesium acetate (TBT/Mg-$(OAc)_2$)[40] or dibutyl tin oxide (DBTO).[41] Each catalyst was employed individually for each of the two different target polymer compositions using BHET as the hard block precursor. The titanium-based catalyst system was exclusively selected for path B (rPET precursor) synthesis after analyzing the chromatographic and thermomechanical results of products from path A.

Alternatively, in the small-scale deconstruction experiments (path B, rPET precursor) the target soft block content was fixed at 52 wt %, and the effect of adding either large (4× mass equiv with respect to rPET repeating units) or small (1× equiv) quantities of ethylene glycol (EG) depolymerization agent was examined. The EG acts to promote deconstruction, facilitate mixing, and promote the incorporation of the DFA, in what would otherwise be a highly viscous mixture with relatively low concentrations of critical hydroxyl groups. The amount of added glycol is a critical recipe parameter for upscaling to ensure process design in accordance with green chemistry principles, minimizing solvents and starting materials whenever possible.

Soft block content was fine-tuned for the large-scale experiments (path B; 100 g scale) toward maximizing work of extension, in which the findings from small-scale reactions were leveraged. Furthermore, for effective thermoplastic elastomeric behavior, the soft block matrix (DFA) must be tethered by physically cross-linked hard block segments, in this case represented by semicrystalline PET (*vide infra*). The effects of EG and catalyst concentration were also revisited upon upscaling to approach optimal process parameters. An overview of all samples including conditions and catalysts is provided in the Supporting Information (Table S1). All materials were characterized with ^1H and ^{13}C nuclear magnetic resonance (NMR) spectroscopy, size exclusion chromatography (SEC), differential scanning calorimetry (DSC), and tensile testing (see detailed descriptions in the Supporting Information).

Synthesis of TPEEs. The synthesis of TPCs from BHET and Pripol 1009 in the small scale (Scheme 1, path A, 3 g) proceeded through a conventional one-pot two-step transesterification/polycondensation mechanism with continuous removal of the EG that is generated throughout the reaction. The reactions were performed in the melt in a small round-bottom flask (10 mL) connected to a dry condenser, which was heated with a heating wire to drive condensate removal (Figure S1). A Teflon-coated magnetic stirring bar was used; gradual build-up of viscosity and the eventual cessation of magnetic stirring provided qualitative evidence, suggesting the formation of a high-molar-mass product.

Equivalent reactions were performed with BHET being replaced by rPET pellets/nurdles (Scheme 1, path B, see the Supporting Information for detailed descriptions of starting materials). The deconstruction of rPET pellets under similar conditions (i.e., small scale) presented several challenges; high-molar-mass material was ultimately unattainable when starting from pellets. First, rPET pellets have a relatively low surface-to-volume ratio compared with the BHET powder. The difference significantly limits the interface between the polymer pellets and EG, which, in turn, results in kinetically retarded glycolysis. Second, the initially transparent rPET pellets became opaque at elevated temperatures (ca. 200 °C), indicating crystallization. Limited permeation of EG in the tightly packed crystalline domains further hindered the molecular deconstruction of rPET. To circumvent these issues, rPET pellets were dissolved in a mixture of $CHCl_3$/trifluoroacetic acid (TFA) (90:10 v/v) and precipitated in MeOH to yield a macroporous solid with increased surface area. Note that this procedure was clearly not intended for scale-up and was merely used in the small-scale reactions to establish the reactivity between the reactants. This procedure was unnecessary in the scaled reactions (*vide infra*). Deconstruction was notably faster in small-scale experiments for an initial feed of 4× the mass equiv of EG with respect to rPET; a homogeneous melt formed in less than 10 min as contrasted with more than 30 min for the 1× EG mass equiv runs. This discrepancy was attributed to the intricacies of the reaction setup: the reflux of EG and homogenization of the reactants was facilitated by intermittently heating (>200 °C) the parts of the flask that were not in contact with the aluminum heating block (Figure S1). Inevitably, this manipulation led to significant amounts of the volatile deconstruction agent (EG) being transferred to the collection flask for the 1× equiv runs. Smaller quantities of EG in the reaction mixture ultimately slows the reaction.

https://doi.org/10.1021/acs.macromol.1c02338
Macromolecules 2022, 55, 1042−1049

Table 1. Summary of Molecular and Thermal Characterization of TPCs

	T_g (°C)[a]	T_c (°C)[a]	ΔH_c (J/g)[a]	T_m (°C)[a]	ΔH_m (J/g)[a]	mol % SB[b]	wt % SB[b]	α_c tot. (%)[c]	HB α_c (%)[c]	LHS[d]	LSS[d]	R[d]	M_n (g/mol)[e]	$Đ$[e]
SB49-BHET-D	−14	104	13.4	201	19.3	22.4	47.7	13.8	26.4	4.8	1.3	1.0	19 800	3.1
SB49-BHET-T	−12	101	15.2	201	20.3	23.1	48.7	14.5	28.2	4.8	1.2	1.0	29 600	2.7
SB60-BHET-D	−20	94	11.5	170	10.7	32.6	60.4	7.6	19.3	3.3	1.4	1.0	23 700	3.9
SB60-BHET-T	−24	101	12.2	170	11.7	31.6	59.4	8.3	20.5	3.4	1.4	1.0	24 900	2.9
SB52-E1-ss	−20	92	9.3	182	15.2	24.9	51.2	10.9	22.2	4.1	1.2	1.1	19 700	2.7
SB52-E4-ss	−21	139	12.2	186	10.4	25.2	51.6	7.5	15.4	4.1	1.3	1.0	22 500	3.0
SB66-E1-ls	−26	84	3.9	145	7.2	37.7	65.7	5.2	15.0	2.8	1.5	1.0	40 500	3.2
SB66-E4-ls	−24	97	2.6	153	4.3	38.1	66.1	3.0	8.9	2.9	1.6	1.0	35 800	3.1

[a]Thermal transitions and enthalpy values obtained from DSC thermograms. [b]Composition determined from integration of signals from ^{1}H NMR spectra. [c]Crystallinity calculated from the composition and melting enthalpy values in reference to melting enthalpy of fully crystalline PET (ΔH_m^0 = 120 J/g)[46] by $\alpha_c = \Delta H_m/\Delta H_m^0$. [d]Segment lengths and randomness determined from ^{13}C NMR spectra. [e]M_n and $Đ$ determined from SEC in $CHCl_3$ at 35 °C, relative to polystyrene standards.

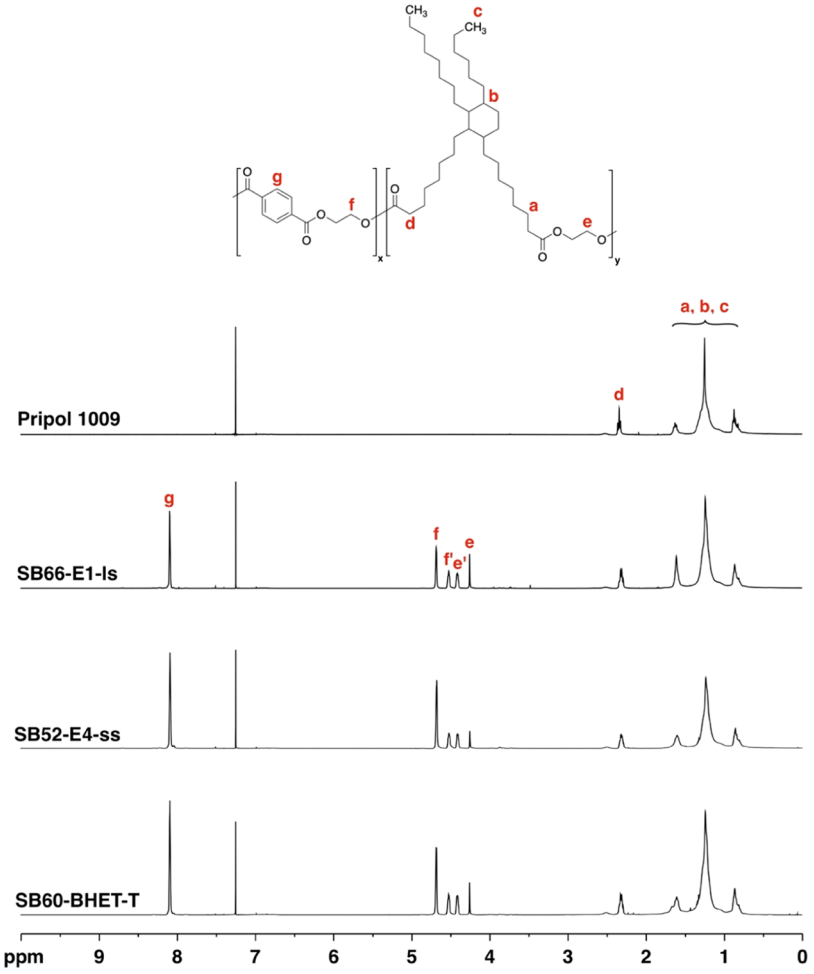

Figure 1. Representative ^{1}H NMR spectra of TPCs synthesized from each synthesis path and macromonomer Pripol 1009 for comparison.

The inherent shortcomings (e.g., precipitation using hazardous solvents) associated with small-scale reactions were largely circumvented by employing a larger-scale custom-built reactor. This reactor consists of a Kugelrohr drying tube oriented vertically as the reaction vessel (1 L internal volume; up to 200 g batch contents possible; Figure S2). The tubular reactor was jacketed with a Kugelrohr heating mantle, which provided homogeneous distribution of heat and allowed for the direct feeding of rPET pellets, while the shape of the reaction vessel ensured that the pellets were constantly submerged in EG. Losses of EG are minimized by the efficient reflux achieved through judicious reactor design. Consequently, the deconstruction kinetics with 1× equiv of EG proved indistinguishable from those with 4× equiv on the large scale. Finally, the *in situ* monitoring of melt viscosity (via torque) provides relative control over the terminal molar mass and enables greatly improved reproducibility compared with small-scale reactions.

Molecular Analysis of TPEEs. A range of samples was generated using the different pathways and having various target compositions, as indicated in the sample names (Table 1). For example, SB66-E1-ls refers to a sample with a rPET hard block precursor, a target soft block content of 66 wt %

https://doi.org/10.1021/acs.macromol.1c02338
Macromolecules 2022, 55, 1042−1049

using an excess of 1× equiv of EG, performed on the large-scale reactor. The composition of TPCs was elucidated with ^{1}H NMR spectroscopy (Figure 1). Measured compositions were very close to target values in all cases, consistent with the efficient incorporation of Pripol 1009 DFA. Results from path A using a BHET hard block precursor suggest a negligible correlation between the catalyst and the composition according to ^{1}H NMR spectra (Figure S3). The average sequence length of a TPC is a key determinant of mechanical properties. Sequence length is routinely probed with ^{13}C NMR spectroscopy.[42,43] In a fully randomized copolymer, both blocks attain their minimum average length and the degree of randomness, R, can be calculated according to established equations (see the Supporting Information). The EG peaks in the hard block, soft block, and interface were identified in the 61−64.5 ppm range (Figure S4). Calculated values of R were very close to unity for all samples. This would suggest that rPET is nearly fully digested into low-molar-mass fragments, which are further lysed by ethylene glycol esters of the Pripol 1009 DFA. The resulting oligomeric copolyesters adopt a statistical segment distribution during the subsequent polycondensation stage. In other words, conspicuously long segments (i.e., blockiness) from an incomplete molecular deconstruction of rPET were not identified with ^{13}C NMR spectroscopy. The segment distributions are consistent with extensive transesterification having occurred in all samples, promoted by the added ethylene glycol. In line with expectations, extensive depolymerization takes place, leading to the redistribution of the ethylene terephthalate units and leading to a segmented copolymer architecture in the final product. This is in line with the relatively high molar mass of the starting rPET material. Essentially, the combined NMR spectroscopic results reveal that TPCs with equivalent molecular make-up can be generated, independent of the nature of the feedstock (i.e., virgin vs waste; monomeric vs polymeric).

On the contrary, SEC measurements reveal marked differences between the molar mass of TPC samples prepared via different methods. The evolution of molar mass is affected predominantly by two parameters, namely, the efficiency of the catalytic system and the removal of EG. According to the Carothers equation, $N_n = (1 - p)^{-1}$, driving the extent of reaction toward completion (conversion, $p = 1$) is critical for attaining high polymers. Removal of EG is promoted by the continual renewal of the interface between the polymer melt and the vacuum environment in the reactor, which is in turn driven by the high-power mechanical stirrer in the large-scale reactor. Consequently, materials made on large scale (ls) have a significantly higher molar mass (Figure 2). The small difference in the molar mass between SB66-E1 and SB66-E4 (40.5 vs 35.8 kg/mol) is ascribed to intrinsic fluctuations in the torque meter during the last stages of polycondensation. The form of the Carothers equation suggests that small differences in reaction time as p approaches unity have a profound influence on N_n. In other words, the discrepancy in molar mass is amplified by small differences in the polymerization extent. The molar mass distributions (i.e., dispersity, $Đ$) for all TPCs are monomodal and consistent with conventional polycondensations. There are low-molar-mass fractions below 1000 g/mol present in all samples, which are presumably ascribed to relatively stable cyclic trimers[44] and dimers[45] of PET. It is important to delineate that the use of the TBT/Mg(OAc) catalyst in path A yielded polymers with higher molar mass as compared to DBTO, which is in turn reflected by the tensile properties (*vide infra*).

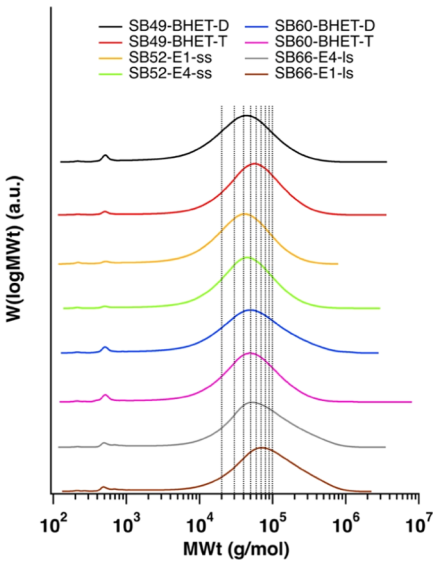

Figure 2. Molecular weight distributions of selected samples from SEC measurements. The low-molar-mass products were clearly separated from the main peak in the chromatograms and were not included in the calculations of M_n and $Đ$. Vertical grid lines have been added between 10^4 and 10^5 g/mol as a visual guide.

Thermal Properties. Unambiguous decreases in both glass transition temperature (T_g) and melting temperature (T_m) with increasing soft block content were observed from thermograms obtained by DSC (Figure 3). The increased molecular mobility of chains richer in the flexible aliphatic DFA component gave rise to a significant reduction in T_g from −12 to −26 °C for TPCs with 49 and 66 wt % soft block, respectively. The T_m follows a similar trend, decreasing from 201 to 145 °C, since the higher aliphatic content also hinders the crystallization of the hard block segments and leads to smaller crystallites. At 66 wt % soft block, the TPCs are nearly at the upper limit of soft block content, above which samples are expected to be fully amorphous, and thus lose the thermoplastic elastomeric character. Melting enthalpies (ΔH_m) were determined from the integration of the melting peaks in thermograms and further used to calculate the approximate degree of crystallinity (α_c) (Table 1). SB66-E1-ls is already on the edge of the semicrystalline limit, exhibiting a degree of crystallinity, α_c = 3.0%, and a minimum degree of crystallinity of the hard block, α_{HB} = 8.9%, among all of the samples. Nevertheless, the low crystallinity was sufficient to impart high toughness to the materials (*vide infra*). The thermograms for the remaining samples are provided in the Supporting Information (Figure S5) and exhibit the same trend in terms of T_g and T_m. Crystallization was observed in nearly all of the samples upon cooling (Figure 3b). Furthermore, cold crystallization (crystallization upon 2nd heating) was observed in several samples, suggesting that increased molecular mobility is required to facilitate equilibrium crystallization. It is clear that the samples with the most soft block (SB66-E1-ls and SB66-E4-ls) have the least crystallization. This is in line with expectations and is consistent with the observations during processing and mechanical evaluation.

Tensile Testing. Samples were melt pressed (180−200 °C) in atmospheric conditions for the preparation of dog bone

https://doi.org/10.1021/acs.macromol.1c02338
Macromolecules 2022, 55, 1042−1049

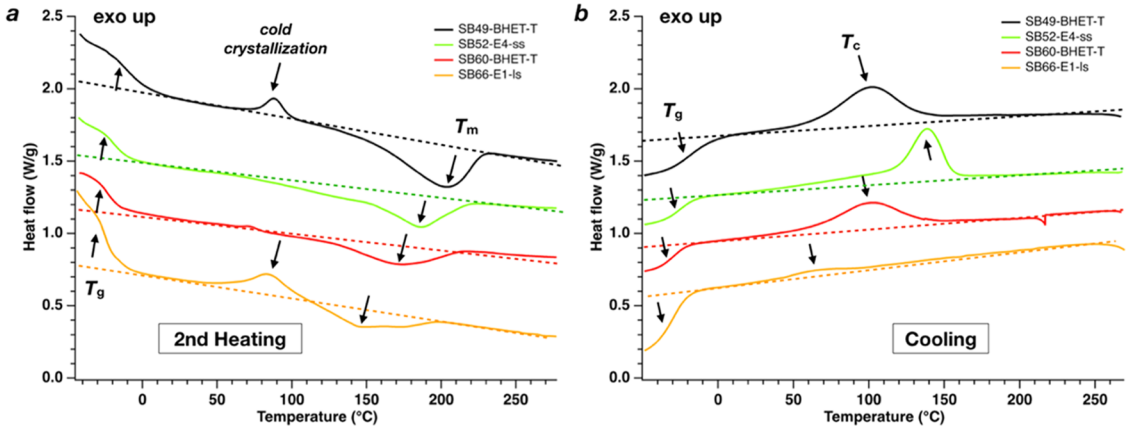

Figure 3. Thermograms for selected samples, showing (a) the second heating cycle and (b) the cooling cycle (10 °C/min) with dashed lines added to indicate approximate baselines to guide the eye. Thermograms have been shifted vertically for clarity, and approximate positions of thermal transitions have been indicated with arrows. Thermogram orientation is exo up.

samples for tensile testing. The samples prepared using small-scale reactions via both synthetic pathways A and B became slightly discolored during melt pressing (Figure S6). We ascribed the discoloration to the presence of residual titanium and magnesium ions from the catalytic system. The mechanism of coloration has been resolved by Van Hoof[47] and was associated with the Ti-catalyzed formation of quinone-type structures under thermo-oxidative conditions. This coloration problem was avoided in the large-scale synthesis by reducing the concentration of TBT down to 100 ppm, yielding transparent and colorless samples (Figure S7a). Notably, directly after melt pressing, the samples appeared transparent, consistent with the low degrees of crystallinity. This is in line with the very low crystallization enthalpies observed from the DSC cooling thermograms. This observation is consistent with expectations for TPCs having PET as a hard block, as opposed to PBT. TPEEs on the market typically contain PBT hard blocks owing to the well-known accelerated crystallization kinetics compared with PET. This renders PET-based TPEEs of limited utility in applications that require injection molding. Further exacerbating this is the fact that the source of rPET in this case (i.e., bottles) has small amounts of co-monomer intended to restrict crystallization. Nevertheless, suitable processing (e.g., thermal annealing treatment) is effective in inducing enough crystallization in these PET-based TPEEs to impart impressive mechanical properties associated with physically cross-linked, segmented morphologies.

Stress−strain plots and a summary bar chart of maximum elongation at break and maximum stress at break provide insight into the molar mass and composition dependence of the mechanics (Figure 4). The accurate determination of Young's modulus, E, is somewhat ambiguous for soft materials since it cannot be defined at the conventional limit of 0.2% strain. This is due to the high extensibility of the TPCs; for this reason, arbitrary values of strain within the limit of small deformations have been taken for the determination of E.[48] The work of extension, U_ε, is provided in the product key, taken as the area underneath the stress−strain curve. Visual inspection of the stress−strain plots for representative samples unequivocally indicates that the stiffness and yield points, σ_y, increase concomitantly with an increase in hard block content. SB66-E1-ls was annealed above its T_c and below its T_m at 120 °C for 1 h, giving rise to sample SB66-E1-ls-an. A modest increase in opacity was observed (Figure S7b), which is

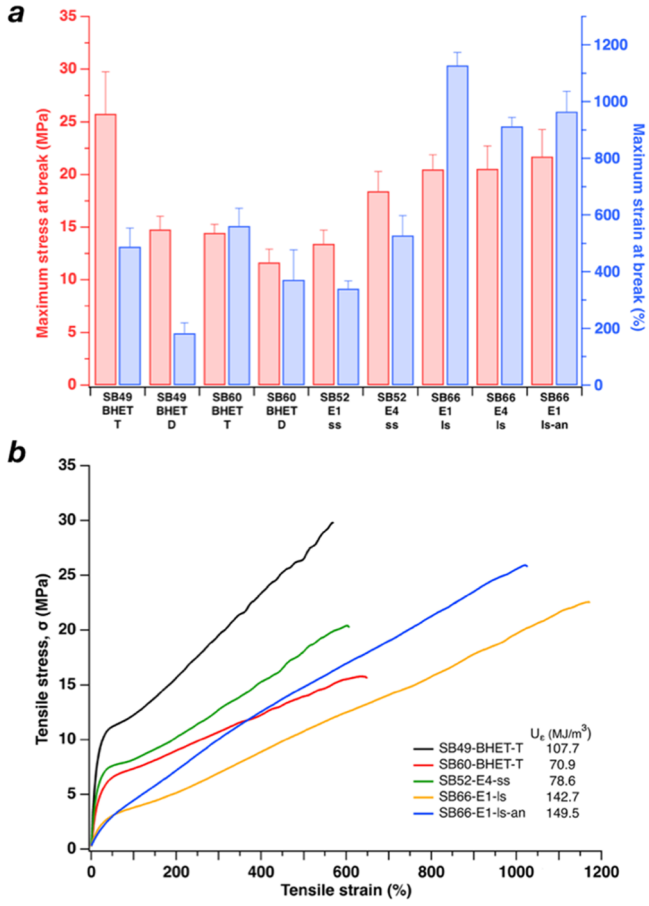

Figure 4. (a) Summary of mechanical properties from tensile tests, maximum stress at break (red), and maximum strain at break (blue). (b) Stress−strain curves for selected samples with work of extension (U_ε) provided in the key.

associated with the formation of dispersed crystallites. Compared to SB66-E1-ls, the annealed SB66-E1-ls-an presents higher stiffness and stress at the break but lower ε_b as a result of the increase in the volume fraction of crystalline domains, which act as physical cross-links. The mechanical properties are consistent with Flory's equation,[49] which relates the ultimate tensile strength of a polymer with its molar mass (UTS = $A - B/M_n$; A, B: constants). The difference in

https://doi.org/10.1021/acs.macromol.1c02338
Macromolecules 2022, 55, 1042−1049

mechanical properties between SB49-BHET-T and -D can be correlated with their M_n (29.6 vs 19.8 kg/mol), in line with the cited relationship. The same rationale holds for SB60-BHET-T and -D, for which the modest difference in M_n resulted in materials with very similar tensile properties. Notably, the mechanical characteristics of SB66-E1-ls (σ_b = 20.5 ± 1.4 MPa and ε_b = 1127 ± 46%) are directly comparable with commercial thermoplastic elastomers such as Dupont's Hytrel RS 40F3 NC010, which contain at least 50 wt % renewably sourced content. Factors that could negate the performance of our waste-sourced materials could be the presence of isophthalic units and/or dye in the rPET pellets, added to hinder PET crystallization after processing, preserve optical clarity and enhance product appearance. Our study demonstrates that rPET waste and a renewable component can be directly combined in a one-pot process for the preparation of high-performance materials. This constitutes an advance compared to protocols where isolation and purification of monomers after chemical recycling are necessary. We believe that this study offers a new paradigm for the responsible use of end-of-life PET and contributes to our efforts for the transition to the circular plastics economy.

CONCLUSIONS

We have demonstrated the synthesis of engineering-grade TPCs using a combination of renewable and postconsumer recycled building blocks via a solvent-free synthetic approach. The scope of the work was twofold: on the one hand, it was shown that high-molar-mass rPET is essentially an equivalent hard block precursor for the synthesis of TPCs, as compared to the monomeric analogue BHET. On the other hand, we have fine-tuned reaction conditions in a batch custom reactor for the one-pot preparation of polymers from responsibly sourced starting materials with mechanical properties directly comparable with commercial TPC analogues. This simple scaling points toward promising applicability in the existing manufacturing infrastructure, which is an intriguing avenue to follow for the future. While the crystallization of PET-based TPEEs appears to be relatively slow, making them unsuitable for applications that require injection molding, the process holds tremendous promise as a platform for making various architectures with alternative feedstocks. We are keen to explore the scope of this strategy further, with other bio-based and postconsumer recycled raw materials. We envision the combination of waste rPET feedstock with an array of diols and sustainable building blocks and are confident that this approach will allow access to a range of TPCs with properties that to date have only been demonstrated via the use of virgin raw materials.

ASSOCIATED CONTENT

Supporting Information

The Supporting Information is available free of charge at https://pubs.acs.org/doi/10.1021/acs.macromol.1c02338.

Additional experimental details, materials, and methods, including photographs of the experimental setup (PDF)

AUTHOR INFORMATION

Corresponding Author

Louis M. Pitet − *Department of Chemistry, Advanced Functional Polymers Laboratory, Institute for Materials Research (IMO), Hasselt University, 3500 Hasselt, Belgium;* orcid.org/0000-0002-4733-0707; Email: louis.pitet@uhasselt.be

Authors

Apostolos A. Karanastasis − *Department of Chemistry, Advanced Functional Polymers Laboratory, Institute for Materials Research (IMO), Hasselt University, 3500 Hasselt, Belgium;* orcid.org/0000-0001-9966-7873

Victoria Safin − *Department of Chemistry, Advanced Functional Polymers Laboratory, Institute for Materials Research (IMO), Hasselt University, 3500 Hasselt, Belgium*

Complete contact information is available at: https://pubs.acs.org/10.1021/acs.macromol.1c02338

Notes

The authors declare no competing financial interest.

ACKNOWLEDGMENTS

The authors greatly appreciate assistance from Greg Quintens (UHasselt) with SEC measurements. We gratefully acknowledge financial support from the Flemish Government and Flanders Innovation & Entrepreneurship (VLAIO) through the Moonshot project CoRe2 (HBC2019.0116). Partial support is also appreciated from Hasselt University and the Research Foundation Flanders (FWO Vlaanderen) via the Hercules project AUHL/15/2-GOH3816N.

REFERENCES

(1) Chamas, A.; Moon, H.; Zheng, J.; Qiu, Y.; Tabassum, T.; Jang, J. H.; Abu-Omar, M.; Scott, S. L.; Suh, S. Degradation Rates of Plastics in the Environment. *ACS Sustainable Chem. Eng.* **2020**, *8*, 3494−3511.

(2) Cheang, C. C.; Ma, Y.; Fok, L. Occurrence and Composition of Microplastics in the Seabed Sediments of the Coral Communities in Proximity of a Metropolitan Area. *Int. J. Environ. Res. Public Health* **2018**, *15*, No. 2270.

(3) Djapovic, M.; Milivojevic, D.; Ilic-Tomic, T.; Lješević, M.; Nikolaivits, E.; Topakas, E.; Maslak, V.; Nikodinovic-Runic, J. Synthesis and Characterization of Polyethylene Terephthalate (PET) Precursors and Potential Degradation Products: Toxicity Study and Application in Discovery of Novel PETases. *Chemosphere* **2021**, *275*, No. 130005.

(4) Wierckx, N.; Prieto, M. A.; Pomposiello, P.; de Lorenzo, V.; O'Connor, K.; Blank, L. M. Plastic Waste as a Novel Substrate for Industrial Biotechnology. *Microb. Biotechnol.* **2015**, *8*, 900−903.

(5) Circular Plastics Alliance. https://Ec.Europa.Eu/Growth/Industry/Policy/Circular-Plastics-Alliance_en (accessed Sept 10, 2021).

(6) Tournier, V.; Topham, C. M.; Gilles, A.; David, B.; Folgoas, C.; Moya-Leclair, E.; Kamionka, E.; Desrousseaux, M.-L.; Texier, H.; Gavalda, S.; Cot, M.; Guémard, E.; Dalibey, M.; Nomme, J.; Cioci, G.; Barbe, S.; Chateau, M.; André, I.; Duquesne, S.; Marty, A. An Engineered PET Depolymerase to Break down and Recycle Plastic Bottles. *Nature* **2020**, *580*, 216−219.

(7) Loop Industries. https://www.loopindustries.com/ (accessed Aug 6, 2021).

(8) Companies are placing big bets on plastics recycling. Are the odds in their favor?. https://cen.acs.org/environment/sustainability/Companies-placing-big-bets-plastics/98/i39 (accessed Aug 11, 2021).

(9) SABIC - Bp And Sabic Embark On New Cooperation For Products From..., https://www.sabic.com/en/news/26431-bp-and-sabic-embark-on-new-cooperation (accessed Aug 11, 2021).

(10) Eastman will build a $250 million plastics recycling plant. https://cen.acs.org/environment/recycling/Eastman-build-250-millionplastics/99/web/2021/02 (accessed Aug 11, 2021).

(11) Vollmer, I.; Jenks, M. J. F.; Roelands, M. C. P.; White, R. J.; van Harmelen, T.; de Wild, P.; Laan, G. P.; Meirer, F.; Keurentjes, J. T. F.;

Weckhuysen, B. M. Beyond Mechanical Recycling: Giving New Life to Plastic Waste. *Angew. Chem., Int. Ed.* **2020**, *59*, 15402−15423.
(12) Thiounn, T.; Smith, R. C. Advances and Approaches for Chemical Recycling of Plastic Waste. *J. Polym. Sci.* **2020**, *58*, 1347−1364.
(13) George, N.; Kurian, T. Recent Developments in the Chemical Recycling of Postconsumer Poly(Ethylene Terephthalate) Waste. *Ind. Eng. Chem. Res.* **2014**, *53*, 14185−14198.
(14) Barnard, E.; Rubio Arias, J. J.; Thielemans, W. Chemolytic Depolymerisation of PET: A Review. *Green Chem.* **2021**, *23*, 3765−3789.
(15) Fukushima, K.; Jones, G. O.; Horn, H. W.; Rice, J. E.; Kato, T.; Hedrick, J. L. Formation of Bis-Benzimidazole and Bis-Benzoxazole through Organocatalytic Depolymerization of Poly(Ethylene Terephthalate) and Its Mechanism. *Polym. Chem.* **2020**, *11*, 4904−4913.
(16) Kim, H. T.; Kim, J. K.; Cha, H. G.; Kang, M. J.; Lee, H. S.; Khang, T. U.; Yun, E. J.; Lee, D.-H.; Song, B. K.; Park, S. J.; Joo, J. C.; Kim, K. H. Biological Valorization of Poly(Ethylene Terephthalate) Monomers for Upcycling Waste PET. *ACS Sustainable Chem. Eng.* **2019**, *7*, 19396−19406.
(17) Kim, D. H.; Han, D. O.; Shim, K. I.; Kim, J. K.; Pelton, J. G.; Ryu, M. H.; Joo, J. C.; Han, J. W.; Kim, H. T.; Kim, K. H. One-Pot Chemo-Bioprocess of PET Depolymerization and Recycling Enabled by a Biocompatible Catalyst, Betaine. *ACS Catal.* **2021**, *11*, 3996−4008.
(18) Fukushima, K.; Liu, S.; Wu, H.; Engler, A. C.; Coady, D. J.; Maune, H.; Pitera, J.; Nelson, A.; Wiradharma, N.; Venkataraman, S.; Huang, Y.; Fan, W.; Ying, J. Y.; Yang, Y. Y.; Hedrick, J. L. Supramolecular High-Aspect Ratio Assemblies with Strong Antifungal Activity. *Nat. Commun.* **2013**, *4*, No. 2861.
(19) Mirjalili, A.; Dong, B.; Pena, P.; Ozkan, C. S.; Ozkan, M. Upcycling of Polyethylene Terephthalate Plastic Waste to Microporous Carbon Structure for Energy Storage. *Energy Storage* **2020**, *2*, No. e201.
(20) Ko, S.; Kwon, Y. J.; Lee, J. U.; Jeon, Y.-P. Preparation of Synthetic Graphite from Waste PET Plastic. *J. Ind. Eng. Chem.* **2020**, *83*, 449−458.
(21) Berkmans, A. J.; Jagannatham, M.; Priyanka, S.; Haridoss, P. Synthesis of Branched, Nano Channeled, Ultrafine and Nano Carbon Tubes from PET Wastes Using the Arc Discharge Method. *Waste Manage.* **2014**, *34*, 2139−2145.
(22) Yuan, X.; Cho, M.-K.; Lee, J. G.; Choi, S. W.; Lee, K. B. Upcycling of Waste Polyethylene Terephthalate Plastic Bottles into Porous Carbon for CF4 Adsorption. *Environ. Pollut.* **2020**, *265*, No. 114868.
(23) Pol, V. G. Upcycling: Converting Waste Plastics into Paramagnetic, Conducting, Solid, Pure Carbon Microspheres. *Environ. Sci. Technol.* **2010**, *44*, 4753−4759.
(24) Tiso, T.; Narancic, T.; Wei, R.; Pollet, E.; Beagan, N.; Schröder, K.; Honak, A.; Jiang, M.; Kenny, S. T.; Wierckx, N.; Perrin, R.; Avérous, L.; Zimmermann, W.; O'Connor, K.; Blank, L. M. Towards Bio-Upcycling of Polyethylene Terephthalate. *Metab. Eng.* **2021**, *66*, 167−178.
(25) Tan, J. P. K.; Tan, J.; Park, N.; Xu, K.; Chan, E. D.; Yang, C.; Piunova, V. A.; Ji, Z.; Lim, A.; Shao, J.; Bai, A.; Bai, X.; Mantione, D.; Sardon, H.; Yang, Y. Y.; Hedrick, J. L. Upcycling Poly(Ethylene Terephthalate) Refuse to Advanced Therapeutics for the Treatment of Nosocomial and Mycobacterial Infections. *Macromolecules* **2019**, *52*, 7878−7885.
(26) Shamsi, R.; Abdouss, M.; Sadeghi, G. M. M.; Taromi, F. A. Synthesis and Characterization of Novel Polyurethanes Based on Aminolysis of Poly(Ethylene Terephthalate) Wastes, and Evaluation of Their Thermal and Mechanical Properties. *Polym. Int.* **2009**, *58*, 22−30.
(27) Demarteau, J.; Olazabal, I.; Jehanno, C.; Sardon, H. Aminolytic Upcycling of Poly(Ethylene Terephthalate) Wastes Using a Thermally-Stable Organocatalyst. *Polym. Chem.* **2020**, *11*, 4875−4882.
(28) Papke, N.; Karger-Kocsis, J. Thermoplastic Elastomers Based on Compatibilized Poly(Ethylene Terephthalate) Blends: Effect of Rubber Type and Dynamic Curing. *Polymer* **2001**, *42*, 1109−1120.
(29) Gioia, C.; Vannini, M.; Marchese, P.; Minesso, A.; Cavalieri, R.; Colonna, M.; Celli, A. Sustainable Polyesters for Powder Coating Applications from Recycled PET, Isosorbide and Succinic Acid. *Green Chem.* **2014**, *16*, 1807−1815.
(30) Baeza, G. P. Recent Advances on the Structure−Property Relationship of Multiblock Copolymers. *J. Polym. Sci.* **2021**, *59*, 2405−2433.
(31) Fray, M. E.; Słonecki, J. Multiblock Copolymers Consisting of Polyester and Polyaliphatic Blocks. *Angew. Makromol. Chem.* **1996**, *234*, 103−117.
(32) Fray, M. E.; Slonecki, J. Dimer Fatty Acid-Modified Poly[Ester-b-Ether]S: Synthesis and Properties. *Polym.-Plast. Technol. Eng.* **1999**, *38*, 51−69.
(33) Manuel, H.; Gaymans, R. Segmented Block Copolymers Based on Dimerized Fatty Acids and Poly(Butylene Terephthalate). *Polymer* **1993**, *34*, 636−641.
(34) Kim, A. R.; Park, M. S.; Lee, S.; Ra, M.; Shin, J.; Kim, Y.-W. Polybutylene Terephthalate Modified with Dimer Acid Methyl Ester Derived from Fatty Acid Methyl Esters and Its Use as a Hot-Melt Adhesive. *J. Appl. Polym. Sci.* **2020**, *137*, No. 48474.
(35) Gubbels, E.; Jasinska-Walc, L.; Merino, D. H.; Goossens, H.; Koning, C. Solid-State Modification of Poly(Butylene Terephthalate) with a Bio-Based Fatty Acid Dimer Diol Furnishing Copolyesters with Unique Morphologies. *Macromolecules* **2013**, *46*, 3975−3984.
(36) Manuel, H. J.; Gaymans, R. J. Segmented Block Copolymers Based on Poly(Butylene Terephthalate) and Telechelic Polyesters and Polyamides of Dimerized Fatty Acids. *Polymer* **1993**, *34*, 4325−4329.
(37) Mukerjee, S. L.; Tabor, R.; Emerson, A. W.; Rogers, K. A.; Vrabel, E. D.; Brown, M. T.; Beatty, M. J.; Kovsky, J. R.; Kellerman, M. D.; Christy, M. R. Polyester Polyols from Thermoplastic Polyesters and Dimer Fatty Acids. WO2015171433A1, November 12, 2015.
(38) Bedell, M.; Brown, M.; Kiziltas, A.; Mielewski, D.; Mukerjee, S.; Tabor, R. A Case for Closed-Loop Recycling of Post-Consumer PET for Automotive Foams. *Waste Manage.* **2018**, *71*, 97−108.
(39) Waskiewicz, S.; Langer, E. Synthesis of New Oligoesterdiols Based on Waste Poly(Ethylene Terephthalate) and Dimerized Fatty Acid. *Polymer* **2021**, *227*, No. 123832.
(40) Witsiepe, W. K. Segmented Polyester Thermoplastic Elastomers. In *Polymerization Reactions and New Polymers*; Platzer, N. A. J., Ed.; Advances in Chemistry; American Chemical Society: Washington, DC, 1973; Vol. *129*, pp 39−60.
(41) Rooney, P. C. Preparation of Polyesters with Tin Catalyst. US5166310A, November 24, 1992.
(42) *Polymer Sequence Determination*; Randall, J. C., Ed.; Academic Press, 1977; pp 41−69.
(43) Japu, C.; Alla, A.; Martínez de Ilarduya, A.; García-Martín, M. G.; Benito, E.; Galbis, J. A.; Muñoz-Guerra, S. Bio-Based Aromatic Copolyesters Made from 1,6-Hexanediol and Bicyclic Diacetalized d-Glucitol. *Polym. Chem.* **2012**, *3*, 2092−2101.
(44) Wei, G.; Wang, L.; Chen, G.; Gu, L. Synthesis and Characterization of Poly(Ethylene-Co-Trimethylene Terephthalate)s. *J. Appl. Polym. Sci.* **2006**, *100*, 1511−1521.
(45) West, S. M.; Smallridge, A. J.; Uhlherr, A.; Völker, S. Small Molecules Accumulated during Polycondensation of Poly(Ethylene Terephthalate). *Macromol. Chem. Phys.* **2000**, *201*, 2532−2534.
(46) Jayakannan, M.; Ramakrishnan, S. Effect of Branching on the Crystallization Kinetics of Poly(Ethylene Terephthalate). *J. Appl. Polym. Sci.* **1999**, *74*, 59−66.
(47) Van Hoof, F. Polyethylene Terephthalate Catalyzed by Titanium (IV) Butoxide. Doctoral Thesis, 2012.
(48) Biemond, G. J. E.; Feijen, J.; Gaymans, R. J. Tensile Properties of Segmented Block Copolymers with Monodisperse Hard Segments. *J. Mater. Sci.* **2008**, *43*, 3689−3696.
(49) Flory, P. J. Tensile Strength in Relation to Molecular Weight of High Polymers. *J. Am. Chem. Soc.* **1945**, *67*, 2048−2050.

https://doi.org/10.1021/acs.macromol.1c02338
Macromolecules 2022, 55, 1042−1049